Structural and Chemical Characteristics of Sisal Fiber and Its Components: Effect of Washing and Grinding

Benítez-Guerrero, M.[a]* , Pérez-Maqueda, L.A.[b], Artiaga, R.[c], Sánchez-Jiménez, P.E.[b], Pascual-Cosp, J.[a]

[a]Departamento de Ingeniería Civil, Materiales y Fabricación, Universidad de Málaga, Dr. Ortiz Ramos Campus Teatinos, Málaga, Spain

[b]Instituto de Ciencia de Materiales de Sevilla, (CSIC -Univ. Sevilla), Sevilla, Spain

[c]Escola Politécnica Superior, Universidade da Coruña, Mendizábal, Ferrol, Spain

Abstract

This work covers the study of microstructural changes of natural sisal fibers induced by different conditioning pretreatments: mechanical grinding, cryogenic grinding and hot water washing. The aim of the work is to clarify the effects of the pretreatments on crystallinity and infrared spectra of sisal. Scanning electron microscopy (SEM) results allowed to identify morphological changes on the fiber surface. Deeper changes, of chemical origin, were studied by attenuated total reflectance (ATR)/Fourier transform infrared spectroscopy (FTIR) and focused on the main components of cellular walls: cellulose, lignin and xylan. The work was complemented with crystallinity index (Ic) data determined by two very different methods: the widely used for lignocellulosic fibers Segal equation based on X-ray diffraction (XRD) measurements, and the one based on FTIR through the 1430/900 cm^{-1} band intensity ratio, which is mostly used with cellulosic samples.

Keywords

Sisal fibers, mechanical grinding, cryogenic grinding, hot water treatment, lignocellulosic components, hydrophilic cotton.

Introduction

Sisal is one of the most widely used lignocellulosic fibers due to its good mechanical properties, low cost and ease of cultivation in arid regions. It was used in a great variety of traditional applications due to its hardness, coarseness and resistance to wear. As other natural lignocelullosic fibers, sisal has gained great interest during the last decades in the manufacturing of composite materials, particularly as reinforcement of mortars, concrete and polymer matrices (Bledzki and Gassan 1999, Li, Mai, and Ye 2000, Satyanarayana et al. 1990).

Each individual sisal fiber is actually a multicellular bundle of polygonal hollow sub-fibers. Cell walls consist of oriented cellulose microfibrils embedded in a matrix, which is composed of lignin and non-cellulosic polysaccharides (NCP), as hemicelluloses and pectins (Barkakaty 1976). Table 1 shows the average composition of sisal fiber. Glucose, mostly from the cellulose fraction, represents a 64.6% of the natural sisal fiber. Other important saccharides are: xylose 15 %, arabinose 2%, galactose 1.4%, manose 1% and rhamnose 0.2%. Lignin accounts for an 11.3%, and uronic acid for a 1.53% (Stewart et al. 1997).

[Table 1 near here]

The optimal use of lignocellulosic materials requires a thorough knowledge on their structural changes caused by conditioning treatments. This work covers a microstructural study of natural sisal fibers, before and after being subjected to hot water washing and two different grinding processes. X-ray diffraction and FTIR spectroscopic methods are used to study the crystallinity and microstructure of the samples, providing additional information regarding the type of components affected by the conditioning treatments.

Experimental

Samples and fibers modifications

Commercial sisal fiber from Brazil was provided by Cayetano García Moral S. L. (Jaén, Spain). The fibers were manually cut to 2-4 mm length, referred here as Natural Sisal. A portion of the Natural Sisal fibers was subjected to the following processes:

i) Grinding in a 120 W blade grinder for 5 min, referred as Sisal MG. ii) Cryogenic impact grinding in a SPEX 6870 Freezer Mill. The treatment consisted of 2 cycles during 2 min at 15 Hz, preceded by a 2 min cooling step by liquid nitrogen. The resulting sample is referred as Sisal CG. iii) Hot water washing. Natural Sisal fibers were submerged into a distilled water bath at 75ºC and were kept under stirring for 2 h. After air drying, this sample is referred as Washed Sisal.

The pure biomass components used were microcrystalline cellulose, alkali low sulphonate content lignin and birch xylan with a minimum xylose content of 90%, all them supplied from Aldrich. Commercial hydrophilic cotton was also used as a representative fiber rich in cellulose.

Equipment and Analytical Techniques

Morphological analysis was performed by SEM, in a low vacuum Hitachi TM-1000 and, previously gold-metalized, in a JEOL SM-6490 LV attached to an EDX Oxford Inca Energy 350 system. Hot water soluble fraction, moisture content and ash content were determined on Natural Sisal and Washed Sisal. Moisture content was obtained by the mass loss on drying method. The sample was weighed, heated in an oven at 110ºC for 4 h, cooled in a desiccator, and reweighed. The ash content was determined by mass loss on calcination, keeping the sample at 800ºC for 4 h. Ashes from Natural Sisal and Washed Sisal were analyzed by XRF in a Panalytical AXIOS. XRD measurements were performed in a Philips X´PertPRO MPD with a X´Celerator RTMS system. Reflection spectra were obtained under Cu $K_{\alpha 1}$ (λ = 1.5406 Å) monochromatic radiation. The mean size of the crystallites, *d*, was

calculated through the Scherrer equation. Chemical structure of the samples was investigated by FTIR spectroscopy in a Bruker Vertex 77. The powdered samples were mixed with KBr and pressed into a disk. A Specac Golden Gate ATR accessory was used for the fiber samples. Spectra were recorded with an accumulation of 32 scans and 4 cm^{-1} resolution in the range from 4000 to 500 cm^{-1}. After baseline correction, sisal, cotton and cellulose spectra were normalized with respect to the relative absorbance maximum, which was located at about 1020-1025 cm^{-1}.

Results

Morphology

Figure 1 shows the morphology of the biomass components and hydrophilic cotton. Natural Sisal and processed sisal fibers are shown in Figures 2 and 3. Figure 2(a) reveals a significant amount of substances adhered to the cell walls of Natural Sisal fibers, including crossing remnants from the spongy parenchimatous cells, which fibers were joined to previously to decortication. The diameter of sisal bundle is not uniform and was observed to vary from 110 to 390 µm in 330 measurements performed on 30 fibers.

[Figure 1 near here], [Figure 2 near here], [Figure 3 near here]

EDX spectroscopy allowed to analyze the composition of the prismatic structures found among ultimate fibers. Figure 2(b) shows some examined regions whose atomic compositions are indicated in Table 2. Calcium is the main component of these structures, associated to calcium oxalate crystals as it is evidenced by XRD, analyzed in a later section. These prismatic structures are better distinguished in backscattered electron micrographs, Figures 2(c) and 2(d), because of their higher Z-contrast.

[Table 2 near here]

Soluble fraction, moisture content, mass loss on calcination and chemical composition of ashes

Table 3 shows the moisture content and mass loss on calcination of Natural Sisal and Washed Sisal, expressed as a percentage of the oven-dry mass of the sample. Chemical composition (wt%) of their ashes is also enlisted, including the predominant oxides (> 1 wt%). It can be observed that calcium is the main component of sisal ashes, followed far behind by magnesium.

The hot water soluble fraction of Natural Sisal is included in Table 3. It is also indicated the percentage of each element removed by hot water washing, expressed as inorganic oxides, ranging from 20 to 94% depending on the cation nature, being discussed afterward.

[Table 3 near here]

FTIR structural analysis

Figure 4 shows the FTIR spectra of cellulose, a linear crystalline polymer composed of D-glucopyranose connected by β-(1,4) linkages (Klemm et al. 1998, Oh, Dong et al. 2005), xylan, a non-crystalline polysaccharide, composed of β-(1,4)-D-xylopyranose units (Marchessault and Liang 1962, Kačuráková et al. 1999), and lignin, an amorphous polymer composed of phenylpropane units bonded by a wide variety of CC and ether linkages, predominant β-O-4 aryl ether bonds. The alkaline lignin analyzed in this work is a G-type, exhibiting specific bands at 1267, 1142, 856 and 817 cm^{-1} associated to conypheryl alcohol or Guaiacyl units (Faix 1991, Sharma et al. 2004).

Figure 5 shows the infrared spectra of Natural Sisal, fibers processed and hydrophilic cotton, whose differences will be further discussed. The main absorption bands of sisal fibers and their assignation to functional groups of biomass components are listed in Table 4. The range below 1800 cm^{-1} corresponds to the fingerprint region, discussed further below.

[Figure 4 near here], [Figure 5 near here], [Table 4 near here]

Comparing with cellulose (Figure 4(a)) and cotton spectra (Figure 5(a)), the absorption bands of sisal fibers located at 1730, 1600, 1425, 1367, 1238 cm^{-1}, and also the weak bands at 1500 and 830 cm^{-1}, correspond to non-cellulosic vibrations, due mainly to the presence of hemicellulose, in addition to pectins, lignin and hydroxycynnamic acids (HCA), p-coumaric and ferulic acids, and a minor proportion of compounds such as lypophilic components found at the sisal cell walls (Gutiérrez, Rodríguez, and Río 2008). Nevertheless, the low lignin content of sisal fiber hinders an accurate assignation of lignin bands (Río et al. 2007). Particularly, the band around 1785-1700 cm^{-1} is mostly associated to non-conjugated C=O stretching of acetyl and acid groups in sisal hemicellulose, but esters and acids groups of phenolic compounds and pectins may also contribute to a lesser extent. The broad band in the 1690-1520 cm^{-1} region is attributed to C=O stretching conjugated with aromatic ring and to C=C stretching of phenolic units, in lignin and HCA compounds, such as ferulic acid (Kačuráková et al. 1999). This band is also contributed by OH bending vibration of adsorbed water, at 1655-1630 cm^{-1} range, and by the antisym COO^- stretching mode of carboxylate groups in uronic acid residues of hemicellulose, in calcium oxalate and in salts of pectic acids. The shoulders and weak bands observed at 1564, 1548 and 1503 cm^{-1} are associated to the aromatic skeleton of phenolic compounds. The bands located at the range 1490-1390 cm^{-1} are assigned to the asym (>1440 cm^{-1}) and sym (<1440 cm^{-1}) CH bending vibrations in different components. The sym COO^- stretching mode of carboxylates also appears in this region, reported to be in around 1430-1400 cm^{-1} for diverse pectates and specifically at 1424 cm^{-1} for calcium pectate (Filippov 1992). The bands in the 1395-1290 cm^{-1} range are due to CH, C-OH bending and OH in-plane deformation vibrations. The main contribution to the absorption band at observed wave number 1367 cm^{1}, of low intensity in cotton fiber, is associated to deformation vibrations of non-cellulosic components of sisal fiber, while the small shoulder around 1334 cm^{-1} and the most intense band located at 1315 cm^{-1}, with larger absorbance in the cotton fiber, are primarily associated to cellulose, in particular to the CH_2 wagging mode (Marchessault 1962). Among the non-cellulosic contributions that could be found in this range, stand out the absorption around 1317 cm^{-1}, characteristic of calcium oxalate salt, and 1328 cm^{-1} associated to the Syringyl ring breathing in the lignin extracted from sisal (Río et al. 2007). The intense band observed at 1238 cm^{-1}, virtually absent in cotton, is largely attributed to the CO stretching vibration of ester groups present in the NCP of sisal fiber. By diffuse reflectance-FTIR spectroscopy it has been reported to appear at a higher wavenumber, 1250 cm^{-1} (Stewart

et al. 1997). Specifically, in pectic substances the CO stretching of methyl esters are located at 1280 and 1220 cm^{-1}, while acetyl esters at 1250 cm^{-1} (Synytsya et al. 2003). The absorbance around 1238 cm^{-1} is also assigned to CO vibrations of ester and ether groups in HCA compounds, which join NCP to lignin. Different studies state that this linkage on certain monocotyledons is mainly accomplished through xylan arabinose chains (Smith and Hartley 1983, Ren and Sun 2010). The strong and wide band between 1186 and 840 cm^{-1} is chiefly due to numerous vibrational modes of cellulose chain, but it is also contributed by vibrations of saccharides in NCP fraction, and to a lesser extent by vibrations associated with certain functional groups of lignin. The absorption bands observed at 1155, 1099 (shoulder), 1025 and 897 cm^{-1}, more prominent in microcrystalline cellulose and hydrophilic cotton than in sisal fiber, are attributed to well established cellulosic vibrations. The first and last ones are assigned to the COC stretching of β-glycosidic linkages in the cellulose and xylan chains of sisal. The most intense peak centered at 1025-1020 cm^{-1} is associated with C-OH, CH and CC stretching vibrations of the different neutral sugars present in sisal fiber. The weak band around 847-800 cm^{-1} might be explained by a low proportion of α-glycosidic links established in saccharide chains, but also by certain phenylpropane units of sisal lignin. In particular, a band at 835 cm^{-1} has been associated to p-hydroxyphenyl building blocks in the lignin extracted from sisal (Megiatto et al. 2007).

Crystallinity Study by X-ray Diffraction

There exist different methods for estimating the proportion of ordered regions in cellulose fibrils, being the equation proposed by Segal one of the most used formula (Segal et al. 1959), $\%I_c = 1 - \frac{I_{am}}{I_{\max}} \times 100$ (1)

where I_{max} is the maximum intensity of the (002) lattice reflection of cellulose I_β type, located at 2ϑ between 22 and 23º, and I_{am} is the intensity attributed to amorphous fraction, given at 2ϑ between 18º and 19º for I_β cellulose. This approach has been extensively employed in the estimation of the crystallinity of lignocellulosic samples (Mwaikambo and Ansell 2002, Paiva and Frollini 2006, Saikia 2008). The estimation of crystallinity index, %Ic(XRD),

consists in comparing the amount of crystalline cellulose respect to the total sample, including both crystalline and amorphous cellulose, lignin, hemicellulose, pectins, etc. (Thygesen et al. 2005).

[Figure 6 near here]

X-ray diffractograms of sisal, cotton and cellulose samples are illustrated as are acquired (Figure 6L) and after normalization (Figure 6R). Monoclinic crystal structure of I_β cellulose allomorph, dominant in higher plants, is observed in all cases. Microcrystalline cellulose presents clear reflections around 2ϑ = 15, 16.5, 20.5, 22.5 and 34.5º (Figure 6(R-d)), corresponding to the planes (101), ($10\bar{1}$), (021), (002) and (040) respectively, also well visible in hydrophilic cotton diffractogram (Figure 6(R-f)). The maximum reflection plane (002) corresponds to the lattice planes of the glycosidic rings, which are the most densely charged structures in cellulose chain. In addition to the peaks around 16, 22.5 and 34.5º distinguished in sisal fibers, X-ray reflections of calcium oxalate monohydrate (pattern 20-0231 JCPDS-ICDD) can be detected, as shown in Sisal MG diffractogram (Figure 6(R-e)). The aggregations observed in SEM micrographs of sisal bundles (Figure 2) are attributed to $CaC_2O_4{\cdot}H_2O$ crystals, responsible of the high calcium content of the sisal ashes.

Table 5 shows the values of %Ic(XRD), estimated by the Segal equation, before and after the correction of scattering effects, resulting in slightly higher values after the count corrections. The crystallinity index of Natural Sisal fiber is close to the values found in literature (Paiva and Frollini 2006, Saikia 2008) and lower than %Ic(XRD) calculated for microcrystalline cellulose and cotton fibers. Crystallite sizes, calculated using the Scherrer formula applied to (002) plane, are listed in Table 5. The values obtained for the different samples of sisal are quite similar (between 24-27 Å), regardless of the sample treatment method, and lower than those of microcrystalline cellulose and cotton fibers (54 and 60 Å respectively).

These results suggest that the various treatments to which the samples were subjected modify the crystallinity index, or the ratio between amorphous and crystalline material, but are not energetic enough to alter the size of cellulose crystallites.

[Table 5 near here]

Crystallinity Study by FTIR study

The relative intensities of the bands located approximately at 1430 and 900 cm^{-1}, sensitive to the crystalline and amorphous cellulose respectively, has been used to quantify the crystallinity or *lateral order index* of cellulose (Oh, Dong et al. 2005) and lignocellulosic fibers (Oudiani et al. 2009). High ratio values indicate that cellulose has a more crystalline and ordered structure, and contrary, a greater bandwidth has been associated to a more disordered structure of cellulose. Table 5 collects the values of *Ic(FTIR)* estimated for sisal, cotton and cellulose samples, according to the method proposed by Oh (Oh, Yoo et al. 2005). There is not a clear correlation between these indices and those calculated by XRD. However, it seems that there is a correspondence between lateral order index and the crystallite size in the cellulosic samples. Thus, the hydrophilic cotton, which has a higher Ic(FTIR) value than microcrystalline cellulose, also has a larger crystallite size. In the case of lignocellulosic samples, the Ic(FTIR) index does not appears to be a good indicator of the crystalline cellulosic fraction, inasmuch as the considered bands are sensitive to the contribution of other biomass components.

Discussion of the effects of grinding and washing treatments on sisal fibers

<u>Effect of mechanical grinding. Sisal MG</u>

It is observed that the mechanical grinding produces the separation of the fiber bundle in its cell ultimate fibers or sub-fibers, which were held together by an amorphous matrix. The cell diameter is between 10 and 28 μm (Figure 3(c)), similar to that of hydrophilic cotton fibers, which is between 7 and 20 μm (Figure 1(d)).

The maximum absorption located at 1024 cm^{-1} in the Natural Sisal ATR spectrum is shifted to about 1030 cm^{-1}. The bands at 1159, 1101 and 897 cm^{-1} appear sharper, and new absorptions can be distinguished at 1047 and 985 cm^{-1} in Sisal MG spectrum, illustrated in Figure 5(d) and better in Figure 7(d).

[Figure 7 near here]

The ratio of peak areas of the Sisal MG bands to those of Natural Sisal, R_{SMG}, was calculated and is presented in Table 4. R_{SMG} values are lower than unity due to the elimination of intercellular components during milling. These data reveal that Sisal MG is enriched in cellulose with respect to Natural Sisal, thus, the ATR spectrum of Sisal MG resembles to that of hydrophilic cotton (Figures 5(a) and 5(d)), except for the presence of characteristic hemicellulosic vibrations at 1727 and 1238 cm^{-1}, mainly associated to the remaining acetyl and acid groups of the O-acetyl-4-O-methylglucuronxylan hemicellulose.

In principle, a gradual increase in crystallinity index could be expected while defibration of the sisal bundle is intensified, since the outcome of treatment is the cellulose microfibrils enrichment. Nevertheless, as it can be observed in Table 5, %Ic(XRD) of Sisal MG is significantly lower than Natural Sisal, but the effect on the crystallite size is small, only a 1 Å difference is discerned with respect to Natural Sisal. The decrease in crystallinity can be explained as consequence of mechanical grinding, which has destroyed the cell walls, thus reducing the crystalline cellulose fraction and increasing the proportion of amorphous intracellular components. A higher decrease might even be observed if some amorphous components of the middle lamella had not been removed during the mechanical grinding.

Effects of cryogenic grinding. Sisal CG

In contrast to mechanical grinding, cryogenic grinding does not produce the separation of the fiber in its cell ultimate fibers, as it shown in Figure 3(d).

Uncorrected %Ic(XRD) values denote a negligible decrease on crystallinity index for sisal fibers cryogenically grinded. The corrected values indicate a slightly larger decrease (Table 5). In any case, the cellulose was not completely amorphizated by the cryogenic treatment.

In contrast, changes in the vibrational spectrum of Sisal CG are more noticeable as compared to the rests of pretreated samples (Figure 5(e)). Its FTIR spectrum shows the highest relative intensity of the vibrations associated with the hydroxyl groups located around 3300 and 1630 cm^{-1}. This effect can be related to an intense moisture

adsorption, as well as to the destruction of bonds and the amorphization of lignocellulosic components. The increase of an active surface area and the defects generated by the cryogenic process could favor the adsorption of humidity from ambient. However, it must be point out that microcrystalline cellulose vibrations remain at 1162, 1120, 1051, 987 and 897 cm^{-1} as observed in Figure 8, where the Sisal CG spectrum is compared with that of microcrystalline cellulose, and better viewed in the inset plot, showing both spectra normalized with respect to the absorbance at 1025 cm^{-1}.

According to these results, cryogenic grinding has been able to generate amorphous material and, simultaneously, purify the cellulose, retaining some degree of crystallinity. The estimated %Ic (XRD) value results from the balance of crystalline cellulose and amorphous components.

[Figure 8 near here]

Effect of hot water washing

Many substances attached to cell walls are removed during the hot washing process, after which the sisal fibers present relatively clean surfaces, as is visible in Figure 3(b). The water-soluble fraction is composed of organic and inorganic compounds and amounts to a 1.9%, as shown in Table 3. The mass loss on calcination of Washed Sisal sample indicates an extraction of inorganic material close to 43%. The results of XRF analysis of ashes (shown in Table 3) reveal that Ca and Mg resist the washing treatment, while Fe and Na are almost completely removed. The different extractability is influenced by both the chemical compounds containing these metals and their accessibility to water during the washing process.

The moisture content of lignocellulosic fibers was reported to depend on their non-crystalline fraction and content of pores (Bledzki and Gassan 1999). The higher humidity percentage of Washed Sisal fibers in relation to Natural Sisal, noted in Table 3, is associated with the removal of hot water soluble substances, which allows a greater exposure to ambient of the hygroscopic components, such as hemicellulose and amorphous cellulose.

The major %Ic(XRD) of Washed Sisal with respect to natural fiber, enlisted in Table 5, can be explained by the pulling out of cellular components of amorphous nature, rather than the increase of cellulose crystallite size, estimated from 25 to 27 Å, produced by the washing process. The subtraction of different water-soluble compounds was verified by ATR. As a consequence of their extraction, Washed Sisal fibers exhibit a series of bands associated with cellulose at 1099, 1055 and 897 cm^{-1}, which are more defined, narrow and acute than those of Natural Sisal, as it is shown in Figure 6(c) and, for a better comparison, in Figure 7(c). The ratio of peak areas respect to Natural Sisal, R_w included in Table 4, allows a better understanding of the changes produced and lets distinguish:

a) Washed Sisal bands with R_w values less than unity, associated to the removal of cell compounds, as: The band located around 2895 cm^{-1} and those in the 1395-1345 cm^{-1} region, mainly the band centered at 1367 cm^{-1}, assigned to CH stretching and bending vibrations respectively.

Bands in the ranges 1685-1555 cm^{-1} and 1490-1395 cm^{-1}, assigned to asymmetric and symmetric stretching vibrations of carboxylate groups, as well as various typical aromatic vibrations. Concretely, the reduction of these relative areas is associated with the extraction of pectic substances and HCA, as well as with the removal of calcium oxalate fragments. The band centered at 1238 cm^{-1}, assigned to CO stretching of ester and ether groups, which are present in NCP and HCA. Finally, it must be highlight the lower relative area of the bands associated with vibrational modes of adsorbed water, in the ranges 3700-3000 and 1650-1630 cm^{-1}, despite the uppermost moisture content of Washed Sisal, noted in Table 3.

b) Bands with R_w values higher than unity, as those in the range 1770-1695 cm^{-1}, associated with stretching modes of carboxylic and ester groups.

The solubility of hemicelluloses depends on its conformation, degree of polymerization (DP), type and degree of substitution (DS) with side chains, as well as, it depends on the presence of acetyl groups, and the existence of linkages with phenolic acids from lignin. A higher degree of substitution facilitates the solubility of a hemicellulose in water, because it decreases the interaction with itself and with cellulose, avoiding the formation of agglomerated

structures of insoluble character (Ren and Sun 2010). A weak interaction with other cellular components appears to be the cause of a better solubility in water (Moers et al. 2005). Specifically, the water extractability of arabinoxylan type hemicelluloses, present in different herbaceous monocots and grasses, resulted to depend on the degree of substitution of arabinose units and on the arabinose/xylose ratio (Izydorczyk, Macri, and A.W. MacGregor 1998, Escarnot et al. 2011). Moreover, it is known that the presence of acetyl groups decreases solubility (Hill, Khalil, and Hale 1998, Tserki et al. 2006). The partial solubility of pectins in aqueous solutions results inversely proportional to their molecular mass (BeMiller 1986) and, apparently, to their degree of esterification (Monsoor and Proctor 2001). Washing can extract pectic uronic acids as pectic carboxylate salts, being the monovalent salts more water-soluble than the di- and trivalent ones (BeMiller 1986). It was also reported that pectins bonded by divalent metal ions such as Ca^{2+} and Mg^{2+} are extracted with cold solutions of chelating agents (Chang, Tsai, and Chang 1993). Indeed, it was observed that these elements are the hardest to remove, with an extraction percentage close to 32 and 20% respectively, as it is collected in Table 3. The extraction of certain carbohydrates from cell walls can also drag phenolic compounds, such as hydroxycynnamic acids. It was documented that lignin-carbohydrate complexes (Sun et al. 1998) and soluble lipophilic compounds (Sun, Salisbury, and Tomkinson 2003) can be extracted by hot water treatment. In accordance with these premises, it can be derived that hot washing enriches sisal fiber in the esterified hemicellulose fraction, presumably containing acetylated groups. This enrichment would occur at the expense of removing a small fraction of hemicellulose, and other low molecular weight compounds, as small carbohydrates and phenolics, such as sugars and HCA, weakly bonded to other cellular components. This agrees with the increase of the band located at 1770-1695 cm^{-1} detected, which should be accompanied by the band centered at 1238 cm^{-1}, whose growth is not perceived due to the inherent extraction of other cellular components containing ether and ester groups, as HCA and pectic substances. Furthermore, removal of hot water soluble substances would explain the decrease in the relative area of the bands centered at 3300 and 1625 cm^{-1}, despite the higher moisture content of Washed Sisal, which in turn would result from the activation and/or generation of physisorption centers after extraction.

Conclusions

The mechanical grinding process leads to the defibration of sisal fibers in its ultimate cells, while cryogenic grinding produces breaking and flattening of the fibers, causing amorphization of the cellulose in different degrees.

Washing in hot water produces partial solubilization of minerals, hemicellulose and other carbohydrates of low molecular weight, such as pectic substances and phenolic compounds as hydroxycinnamic acids, leading to enrichment in hemicellulose containing acetylated groups. After extraction, two effects are evidenced: i) the increase of the moisture absorbed by the fiber, due to a greater number of hydrophilic active groups exposed, and ii) an apparent increase of the crystallinity index %Ic(XRD).

Determination of XRD crystallinity index of samples with three-dimensional structure, such as natural fibers, requires a careful analysis of the results, making use of additional spectroscopic techniques such as FTIR and ATR-FTIR. However, crystallinity index estimated from the 1430/900 band intensity ratio is not adequate for lignocellulosic materials, due to the contribution of other biomass components. Thus, to study cellulosic samples of different origin, comparison of other cellulose characteristic bands in the 1185-845 cm^{-1} range is more elucidating.

The data provided here constitute a foundation for future applications of sisal fiber, such as manufacturing of reinforced composites, as support or skeleton in the synthesis of advanced materials and as a source of specific raw materials for various synthetic processes.

Acknowledgments

Author M. Benítez Guerrero wishes to thank the Spanish Consejo Superior de Investigaciones Científicas (CSIC) for the awarding of a JAE pre-doctoral grant accomplished in the Associated Unit titled "Laboratorio de Materiales and Superficies" (CSIC-Univ. Málaga).

References

Barkakaty, B.C. 1976. "Some structural aspects of sisal fibers." *Journal of Applied Polymer Science* 20:2921-2940.

BeMiller, J.N. 1986. "An introduction to pectins: structure and properties." In *Chemistry and Function of Pectins*, edited by M. Fishman et al., 2-12. Washington DC: American Chemical Society.

Bledzki, A. K., and J. Gassan. 1999. "Composites reinforced with cellulose based fibres." *Progress in Polymer Science* 24: 221-274.

Chang, C.Y., Y.R. Tsai, and W.H. Chang. 1993. "Models for the interactions between pectin molecules and other cell-wall constituents in vegetable tissues." *Food Chemistry* 48:145-157.

Escarnot, E., M. Aguedo, R. Agneessens, B. Wathelet, and M. Paquot. 2011. "Extraction and characterization of water-extractable and water-unextractable arabinoxylans from spelt bran: Study of the hydrolysis conditions for monosaccharides analysis." *Journal of Cereal Science* 53:45-52.

Faix, O. 1991. "Classification of lignins from different botanical origins by FT-IR spectroscopy." *Holzforschung - International Journal of the Biology, Chemistry, Physics and Technology of Wood* 45:21-28.

Filippov, M.P. 1992. "Practical infrared spectroscopy of pectic substances." *Food Hydrocolloids* 6:115-142.

Gutiérrez, A., I.M. Rodríguez, and J.C. del Río. 2008. "Chemical composition of lipophilic extractives from sisal (Agave sisalana) fibers." *Industrial Crops and Products* 28:81-87.

Hill, C.A.S., H.P.S.A. Khalil, and M.D. Hale. 1998. " A study of the potential of acetylation to improve the properties of plant fibres." *Industrial Crops and Products* 8:53-63.

Izydorczyk, M.S., L.J. Macri, and A.W. MacGregor. 1998. "Structure and physicochemical properties of barley non-starch polysaccharides - I. Water-extractable β-glucans and arabinoxylans. ." *Carbohydrate Polymers* 35:249-258.

Kačuráková, M., N. Wellner, A. Ebringerová, Z. Hromádková, R.H. Wilson, and P.S. Belton. 1999. "Characterisation of xylan-type polysaccharides and associated cell wall components by FT-IR and FT-Raman spectroscopies." *Food Hydrocolloids* 13:35-41.

Klemm, D., B. Philipp, T. Heinze, U. Heinze, and W. Wagenknecht. 1998. "Analytical Methods in Cellulose Chemistry." In *Comprehensive Cellulose Chemistry. Fundamentals and Analytical Methods*, 181-195. Weinheim: Wiley-VCH.

Li, Y., Y. Mai, and L. Ye. 2000. "Sisal fibre and its composites: a review of recent developments." *Composites Science and Technology* 60:2037-2055.

Marchessault, R.H. 1962. "Application of infrared spectroscopy to cellulose and wood polysaccharides." *Pure and Applied Chemistry* 5:107-130.

Marchessault, R.H., and C.Y. Liang. 1962. "The infrared spectra of crystalline polysaccharides. VIII. Xylans." *Journal of Polymer Science* 59:357-378.

Megiatto, J.D., W. Hoareau, C. Gardrat, E. Frollini, and A. Castellan. 2007. "Sisal fibers: Surface chemical modification using reagent obtained from a renewable source; characterization of hemicellulose and lignin as model study." *Journal of Agricultural and Food Chemistry* 55:8576-8584.

Moers, K., I. Celus, K. Brijs, C.M. Courtin, and J.A. Delcour. 2005. "Endoxylanase substrate selectivity determines degradation of wheat water-extractable and water-unextractable arabinoxylan." *Carbohydrate Research* 340:1319-1327.

Monsoor, M.A., and A. Proctor. 2001. "Preparation and Functional Properties of Soy Hull Pectin." *Journal of the American Oil Chemists Society* 78:709-713.

Mwaikambo, L., and M. Ansell. 2002. "Chemical modification of hemp, sisal, jute, and kapok fibers by alkalization." *Journal of Applied Polymer Science* 84:2222-2234.

Oh, S.Y., I.Y. Dong, Y. Shin, C.K. Hwan, Y.K. Hak, S.C. Yong, H.P. Won, and H.Y. Ji. 2005. "Crystalline structure analysis of cellulose treated with sodium hydroxide and carbon dioxide by means of X-ray diffraction and FTIR spectroscopy." *Carbohydrate Research* 340:2376-2391.

Oh, S.Y., D.I. Yoo, Y. Shin, and G. Seo. 2005. "FTIR analysis of cellulose treated with sodium hydroxide and carbon dioxide." *Carbohydrate Research* 340:417-428.

Oudiani, A. El, Y. Chaabouni, S. Msahli, and F. Sakli. 2009. "Physico-chemical characterisation and tensile mechanical properties of Agave americana L. fibres." *Journal of the Textile Institute* 100:430-439.

Paiva, J.M.F. De, and E. Frollini. 2006. " Unmodified and modified surface sisal fibers as reinforcement of phenolic and lignophenolic matrices composites: Thermal analyses of fibers and composites." *Macromolecular Materials and Engineering* 291:405-417.

Ren, J.L., and R.C. Sun. 2010. "Hemicelluloses." In *Cereal Straw as a Resource for Sustainable Biomaterials and Biofuels*, 73-130. Amsterdam.

Río, J.C. del, A. Gutiérrez, I.M. Rodríguez, D. Ibarra, and A.T. Martínez. 2007. "Composition of non-woody plant lignins and cinnamic acids by Py-GC/MS, Py/TMAH and FT-IR." *Journal of Analytical and Applied Pyrolysis* 79:39-46.

Saikia, D. 2008. "Investigations on structural characteristics, thermal stability, and hygroscopicity of sisal fibers at elevated temperatures." *International Journal of Thermophysics* 29:2215-2225.

Satyanarayana, K.G., K. Sukumaran, P.S. Mukherjee, C. Pavithran, and S.G.K. Pillai. 1990. "Natural fibre-polymer composites." *Cement and Concrete Composites* 12:117-136.

Segal, L., J.J. Creely, A.E.J. Martin, and C.M. Conrad. 1959. "An empirical method for estimating the degree of crystallinity of native cellulose using the X-ray diffractometer." *Textile Research Journal* 29:786-794.

Sharma, R.K., J.B. Wooten, V.L. Baliga, X. Lin, W.G. Chan, and M.R. Hajaligol. 2004. "Characterization of chars from pyrolysis of lignin." *Fuel* 83:1469-1482.

Smith, M.M., and R.D. Hartley. 1983. "Occurrence and nature of ferulic acid substitution of cell-wall polysaccharides in graminaceous plants." *Carbohydrate Research* 118:65-80.

Stewart, D., A. Azzini, A.T. Hall, and I.M. Morrison. 1997. "Sisal fibres and their constituent non-cellulosic polymers." *Industrial Crops and Products* 6:17-26.

Sun, R., J.M. Fang, A. Goodwin, J.M. Lawther, and A.J. Bolton. 1998. "Fractionation and characterization of polysaccharides from abaca fibre." *Carbohydrate Polymers* 37:351-359.

Sun, R.C., D. Salisbury, and J. Tomkinson. 2003. "Chemical composition of lipophilic extractives released during the hot water treatment of wheat straw." *Bioresource Technology* 88:95-101.

Synytsya, A., J. Čopíková, P. Matějka, and V. Machovič. 2003. "Fourier transform Raman and infrared spectroscopy of pectins." *Carbohydrate Polymers* 54:97-106.

Thygesen, A., J. Oddershede, H. Lilholt, A.B. Thomsen, and K. Ståhl. 2005. "On the determination of crystallinity and cellulose content in plant fibres." *Cellulose* 12:563-576.

Tserki, V., P. Matzinos, N.E. Zafeiropoulos, and C. Panayiotou. 2006. "Development of biodegradable composites with treated and compatibilized lignocellulosic fibers." *Journal of Applied Polymer Science* 100:4703-4710.

Yu, C. 2005. "Sisal." In *Bast and Other Plant Fibres*, edited by R.R. Franck, 304-304. Cambridge: Woodhead.

Tables

Table 1 Compositional ranges of sisal fiber

Component	Compositional Range (wt%)
Cellulose	43-88
Hemicellulose	10-15
Lignin	4-20
Pectin	0.8-10
Water soluble	1-4
Fat and wax	0.15-2
Moisture	10-22

Table 2 Chemical composition, determined by EDX, of the selected areas in Figure 2(b).

Element (wt%)	Spectrum 1	Spectrum 2	Spectrum 3	Spectrum 4
C	5.04	5.43	7.41	17.95
O	14.42	13.43	6.63	19.77
Mg	0.03	a	a	a
Si	0.04	a	a	a
Ca	6.15	5.78	a	a

a No detected

Table 3 Moisture, loss on calcination and chemical composition of the Natural Sisal and Washed Sisal samples.

		Natural Sisal	Washed Sisal	% Extraction *
Humidity %		9.68	11.23	
Water soluble fraction %				1.86
Calcination loss %		99.33	99.62	
Ash (wt%)	CaO	65.13	78.54	*32*
	MgO	10.60	14.92	*20*
	Na_2O	5.97	0.76	*93*
	SiO_2	4.81	1.57	*81*
	Fe_2O_3	4.15	0.45	*94*
	SO_3	3.02	1.50	*72*
	Al_2O_3	2.70	0.73	*85*
	P_2O_5	1.87	0.84	*74*
	K_2O	1.74	0.67	*78*

* It refers to the lixiviated fraction by hot washing. The water soluble fraction was determined empirically and the oxide lixiviation percentage (in cursive) was calculated by knowing ash content and oxide composition of the raw and washed sisal.

Table 4. Band assignation for the ATR-FTIR spectrum of sisal

Range (cm^{-1})	R_{SMG} [a]	Rw [b]	Characteristic wavenumber (cm^{-1})			Peak assignment
			Natural S	Sisal MG	Washed S	
3700-3000	0.53	0.88	3284	3328	3323	O-H stretching intramol. And intermolecular H bridge between OH groups
2980-2800	0.56	0.80	2893	2891	2895	Alquil aliphatic C-H stretching
1770-1695	0.89	1.31	1727	1727	1730	C=O stretching of esters (COOR), carboxylic acids (COOH, ketones, etc. (NCP, lignin and HCA)
			1625 sh	1629	1625 sh	Adsorbed water
1685-1555	0.49	0.85	1597	1597	1597	C=O and C=C stretching (lignin and HCA) Asymmetric stretching COO^- (NCP)
1565-1490			1498	1498	1503	Aromatic ring vibrations (lignin and HCA)
				1450	1450 sh	CH asymmetric bending
1490-1395	0.61	0.90	1425	1425	1425	C=C aromatic ring vibrations (lignin and HCA) CH symmetric bending Symmetric stretching COO^- (NCP)
1395-1345	0.68	0.87	1367	1367	1367	CH symmetric bending
1345-1290	0.84	0.98	1315	1334 sh 1315	1334 sh 1315	CH_2 wagging (cellulose)
1290-1185	0.79	0.96	1238	1238	1238	C-O stretching
			1155	1159	1155	C-O-C stretching at glycosidic link
			1099 sh	1101	1099	C-OH stretching
1185-845	0.94	1.06	1024	1047 sh 1030 985	1055 sh 1022	C-C and C-O stretching C-OH, C-O and C-C stretching
			897	897	897	C-O-C stretching at glycosidic link
840-800			830	830	830	p-hydroxyphenyl units (lignin)

NCP, Non cellulosc polymers; HCA, Hydroxycinnamic acids; Sh, shoulder.

a Ratio area Sisal MG / Natural Sisal (R_{SMG})

b Ratio area Washed Sisal / Natural Sisal (Rw)

Table 5 Values of %Ic, determined by different methods, and crystallite size of untreated and treated Sisal fibers, hydrophilic cotton and micro-crystalline cellulose

	Ic% (XRD) [a]	Ic% (XRD) [b]	d(Å) [c]	Ic (FTIR) [d]
Microcristalline cellulose	66.5	71.9	54	2.56
Hydrofilic cotton	68.5	69.1	60	3.43
Natural Sisal fibre	60.0	64.6	25	3.54
Sisal MG	46.0	47.5	24	1.91
Sisal CG	59.6	61.9	26	e
Washed Sisal fibre	64.3	69.7	27	2.63

a Determined by Segal equation

b Determined by Segal equation after counts correction

c Calculated by Scherrer equation at (002) plane

d Determined as ratio Abs(1425/897)

e Too low band intensity to calculate *Ic(FTIR)*

Figures

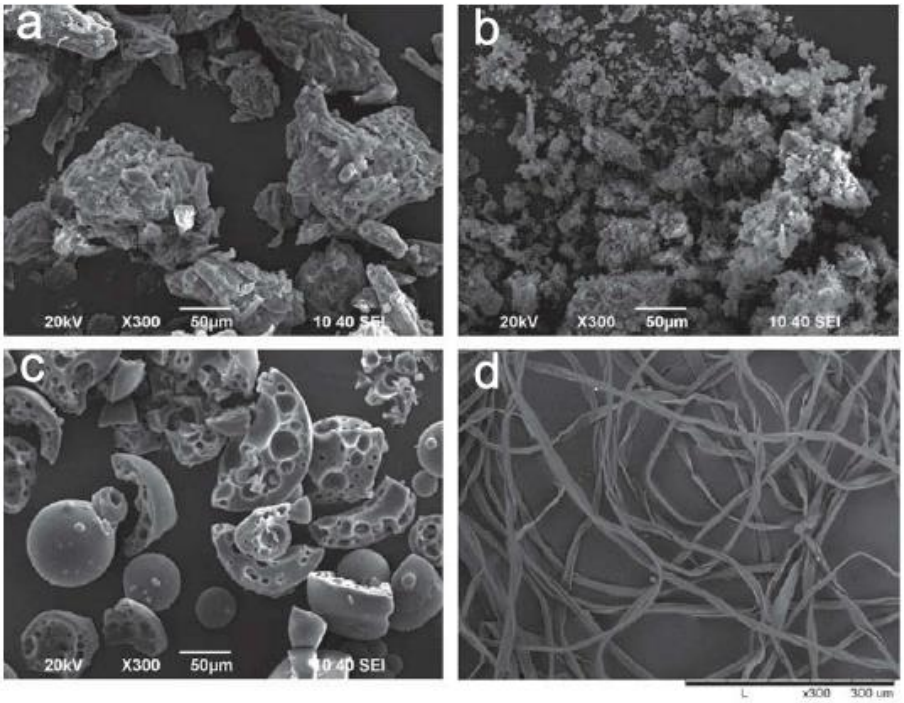

Figure 1. SEM micrographs of the main sisal biocomponents and hydrophilic cotton: microcrystalline cellulose (a), xylan (b), lignin (c), hydrophilic cotton (d).

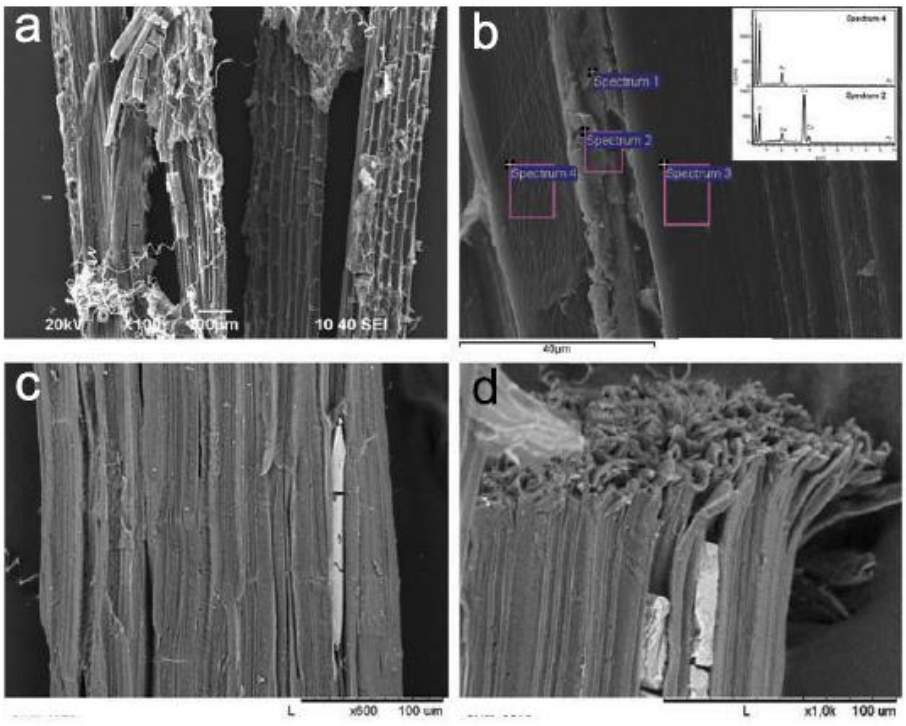

Figure 2. SEM micrographs of Natural Sisal: general structure observed at 100X (a), regions where EDX analysis was performed (b), region of the fiber containing a mineral deposit (c), end of the fiber containing mineral deposits (d).

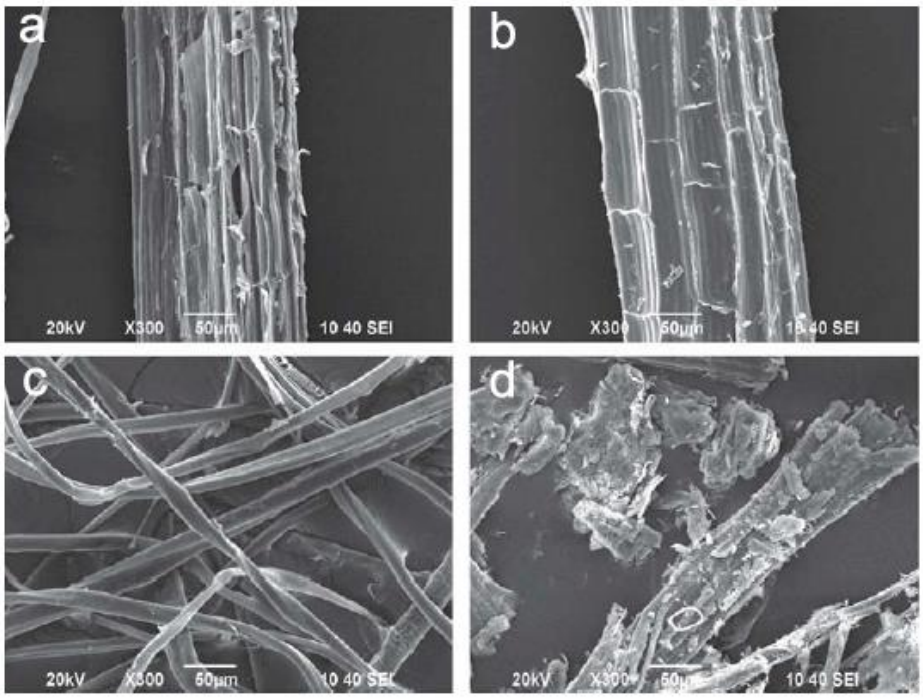

Figure 3. SEM micrographs of the different sisal samples: Natural Sisal (a), Washed Sisal (b), Sisal MG (c), Sisal CG (d).

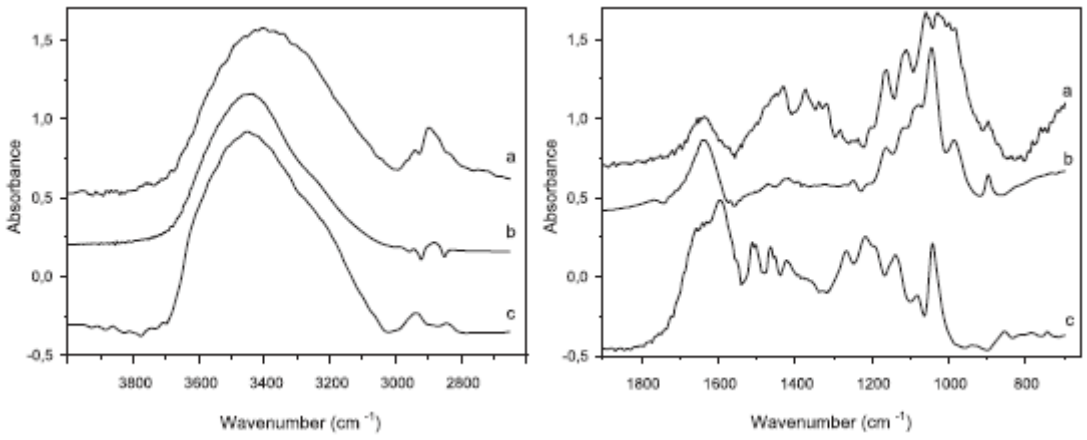

Figure 4. FTIR spectra of microcrystalline cellulose (a), xylan (b), and lignin (c).

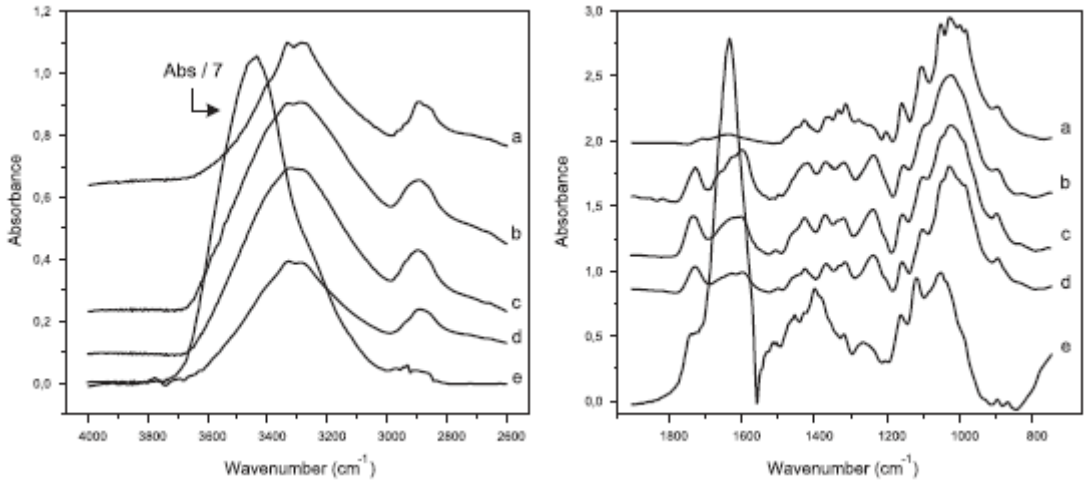

Figure 5. Normalized ATR-FTIR spectra of hidrophillic cotton (a), Natural Sisal (b), Washed Sisal (c), Sisal MG (d) and Sisal CG (e). For a better comparison, absorbance of Sisal GC was divided by 7 in the 4000-2800 cm^{-1} range.

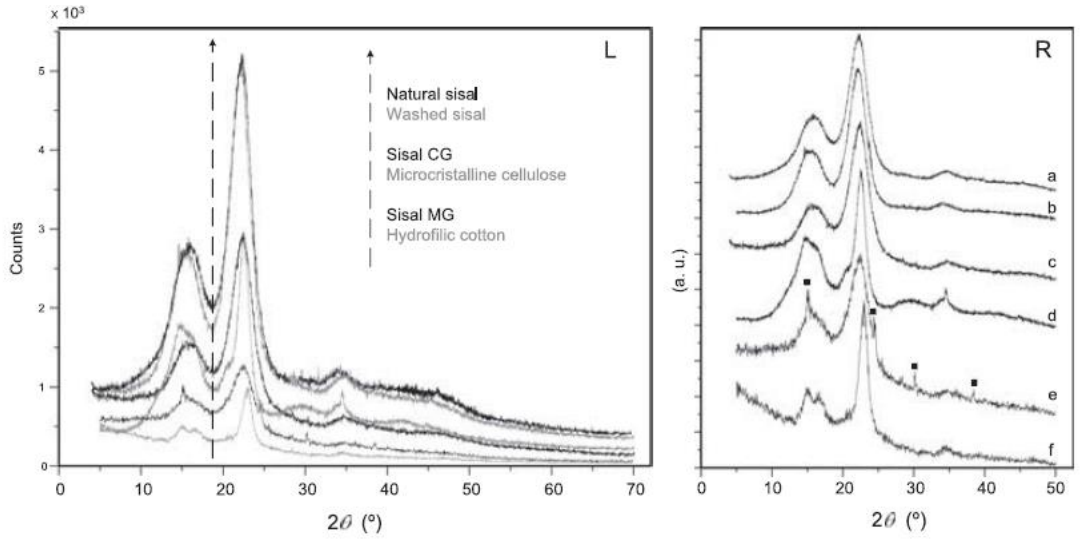

Figure 6 (L). X-ray diffraction patterns of the samples: Natural Sisal (a), Washed Sisal (b), Sisal CG (c), microcrystalline cellulose (d), Sisal MG (e), and hydrophillic cotton (f). Figure 6 (R). Normalized X-ray diffraction patterns.

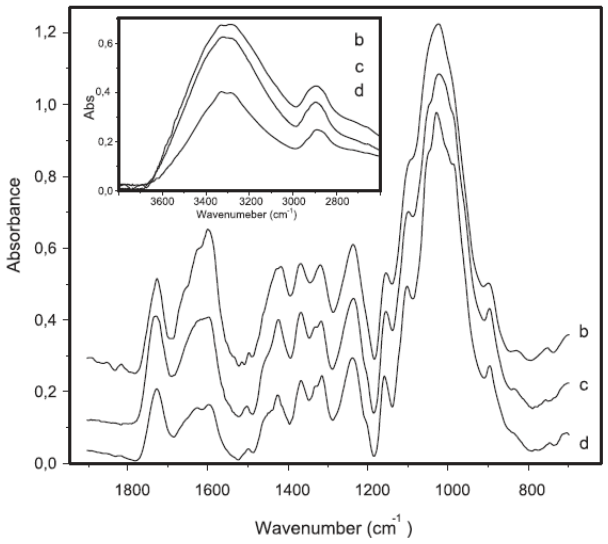

Figure 7. Overlay of the normalized ATR-FTIR spectra of Natural Sisal (b), Washed Sisal (c), and Sisal MG (d).

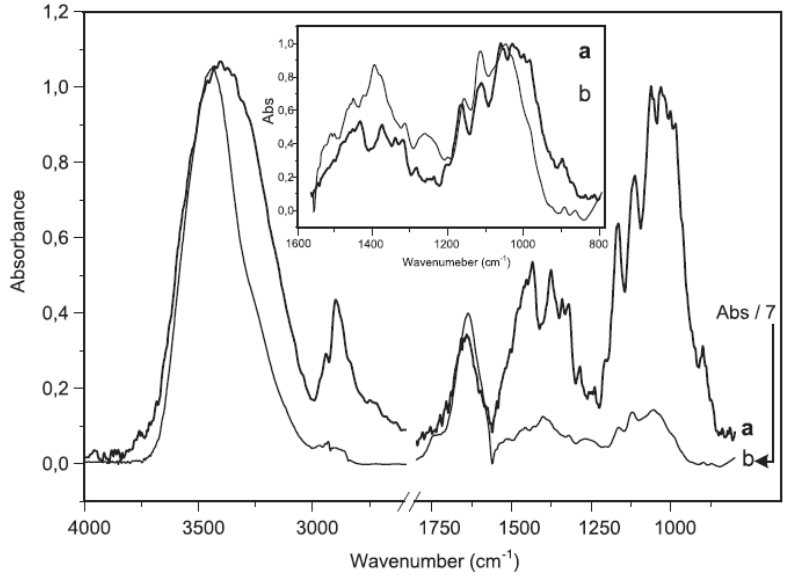

Figure 8. Overlay of the FTIR spectra of microcrystalline cellulose (a) and Sisal CG (b). Absorbance of Sisal CG was divided by 7 for a better comparison. The inset shows the spectra, normalized at 1025 cm^{-1}, in the range from 1550 to 800 cm^{-1}.